Check for updates

9-cis-Neoxanthin in Light Harvesting Complexes of Photosystem II Regulates the Binding of Violaxanthin and Xanthophyll Cycle[1][OPEN]

Ke Wang[2], Wenfeng Tu[2], Cheng Liu, Yan Rao, Zhimin Gao, and Chunhong Yang*

Key Laboratory of Photobiology, Institute of Botany, Chinese Academy of Sciences, Beijing 100093, China (K.W., W.T., C.L., Y.R., C.Y.); University of the Chinese Academy of Sciences, Beijing 100049, China (K.W.); and Key Laboratory on the Science and Technology of Bamboo and Rattan, International Center for Bamboo and Rattan, Beijing 100102, China (Z.G.)

ORCID ID: 0000-0003-1087-8135 (C.Y.).

The light-harvesting chlorophyll *a/b* complex of photosystem II (LHCII) is able to switch to multiple functions under different light conditions (i.e. harvesting solar energy for photosynthesis and dissipating excess excitation energy for photoprotection). The role of the different carotenoids bound to LHCII in regulating the structure and function of the complex is a long-lasting question in photosynthesis research. 9-cis-Neoxanthin (Nx) is one of the important carotenoids, which can only be found in the LHCIIs. High-resolution structural analysis of LHCII shows that Nx is located between different monomeric LHCIIs, with one side protruding into the lipid membrane. In this study, the various functional significances of this unique feature of Nx binding in LHCII are studied with the in vitro reconstituted LHCIIs both with and without Nx and the native complexes isolated either from wild-type Arabidopsis (*Arabidopsis thaliana*) or from its mutant *aba4-3* lacking Nx. Our results reveal that the binding of Nx affects the binding affinity of violaxanthin (Vx) to LHCII significantly. In the absence of Nx, Vx has a much higher binding affinity to trimeric LHCII. The strong coordination between Nx and Vx at the interfaces of adjacent monomers of LHCII plays an important role both in operating the xanthophyll cycle and in the transient modulation of nonphotochemical quenching.

The light-harvesting complex of PSII (LHCII) is a multifunctional membrane protein that plays important roles in regulating the functions of the thylakoid membrane under different environmental conditions. Under moderate light, LHCII absorbs solar light and transfers the excitation promptly to the reaction center. Upon overexcitation, it dissipates the absorbed excess energy to protect the photosynthetic apparatus from photodamage. The mechanisms of the switch of LHCII between these two different states, as well as its structural basis, are long-lasting questions that are still debated (Ruban, 2015).

A unique feature of LHCII is its abundant photon-absorbing cofactors that form an extensive network for the highly efficient harvest and transfer of solar energy in spite of the extremely high pigment concentration in the thylakoid membranes. Besides the 14 chlorophylls (Chls), each LHCII monomer binds four carotenoid (Car) molecules, namely two lutein (Lut), one 9-cis-neoxanthin (Nx), and one violaxanthin (Vx; Liu et al., 2004; Standfuss et al., 2005). The two Lut at the L1 and L2 sites, located at the center of LHCII, possess the highest binding affinities to LHCII among all the Cars. Nx, although connected with only one hydrogen bond with a luminal-loop residue, Tyr-112 (N1), has a relatively high binding affinity via the hydrophobic interaction with the Chl*b* cluster. In contrast, Vx has the lowest binding affinity to LHCII. Isolation of the LHCII complexes with the mildest detergent yielded only 0.2 Vx per monomer (Ruban et al., 1999).

Cars are very important for LHCII, not only in stabilizing the structure of LHCII but also in regulating the efficiency of excitation energy usage (Croce et al., 1999; Ruban et al., 2007; Kirilovsky, 2015). The Lut at the L1 site regulates the energy transfer to the end emitter Chl*a* (Ruban et al., 2007), while that at L2, located with one end in the Chl*b*-rich region, ensures a close interaction between Chl*a* 604 and Nx, which is ultimately important in regulating the triplet energy distribution in LHCII (Zhang et al., 2014). Nx, with its unique 9-cis

[1] This work was supported by the Strategic Priority Research Program of the Chinese Academy of Sciences (grant no. XDB17030100) and the National Natural Science Foundation of China (grant nos. 31370275, 31570236, 31600192, and 31370588).

[2] These authors contributed equally to the article.

* Address correspondence to yangch@ibcas.ac.cn.

The author responsible for distribution of materials integral to the findings presented in this article in accordance with the policy described in the Instructions for Authors (www.plantphysiol.org) is: Chunhong Yang (yangch@ibcas.ac.cn).

K.W., W.T., C.L., and Y.R. performed experiments; Z.G. provided the VDE reaction system; K.W. and C.Y. designed this study and wrote the article; K.W., W.T., and C.Y. analyzed the data; all authors discussed the results and commented on the article.

[OPEN] Articles can be viewed without a subscription.

www.plantphysiol.org/cgi/doi/10.1104/pp.17.00029

Downloaded from on October 18, 2017 - Published by www.plantphysiol.org
Copyright © 2017 American Society of Plant Biologists. All rights reserved.

configuration, located at the periphery of LHCII and in the Chl*b* region, is involved in scavenging the singlet oxygen produced under overexcitation conditions (Dall'Osto et al., 2007). Vx, also located peripherally but distant from the Nx of the same monomer, is a component of the xanthophyll cycle, as the substrate for violaxanthin deepoxidase (VDE), which converts Vx to antheraxanthin and zeaxanthin (Zx). Because of its longer conjugated double bond chain, Zx is able to accept excitation from Chl and to dissipate the harmful excessive energy as heat (Holt et al., 2005).

The two peripherally located Cars (Vx and Nx) possess unique regulatory mechanisms in executing their functions. The most unstable bound Car, Vx, when functioning as a substrate of VDE, is liberated from LHCII and transferred to the lipid phase on the lumenal side of the thylakoid membrane for deepoxidation. Although the characteristics of VDE were discovered long ago, the regulatory mechanism whereby Vx dissociates from LHCII remains unclear (Jahns et al., 2009). Nx, a biosynthetic precursor for abscisic acid (Oritani and Kiyota, 2003), is the only Car in the photosynthetic apparatus that is cis-configured (Liu et al., 2004). This isomer exists only in PSII of Chl*a*/*b*-containing chloroplasts (Caffarri et al., 2007), while all-trans-neoxanthin also can be found in petals or fruits (Takaichi and Mirauro, 1998). The phylogeny of photosynthesis indicates that the appearance of Nx coincides with that of Chl*b*, which may be related to the fact that Nx is closely associated with Chl*b* (Takaichi and Mirauro, 1998). It was observed that a lack of Nx in the Arabidopsis (*Arabidopsis thaliana*) mutant *aba4-1* influenced neither the excitation energy transfer, nor the harmful energy dissipation, nor the luminal-loop conformation, although it did show the reduced scavenging of singlet oxygen under excessive light (Dall'Osto et al., 2007; Mozzo et al., 2008; Fehr et al., 2015). It is proposed that Nx undergoes conformational change that is indirectly related to the nonphotochemical quenching (NPQ) in LHCII, because it is the basis for allosteric adjustment between unquenched and quenched states under different environmental conditions (Ruban et al., 2007; Ilioaia et al., 2008). Nx displays special binding characteristics, and its binding to LHCII is thermodynamically reversible (Hobe et al., 2006), which is suggested to be involved in the reorganization of the photosynthetic membrane supercomplexes that is essential for the adaptation of the photosynthetic membrane to the changing environment. Dynamic molecular modeling indicates that the variations of the interactions between the hydrogen bond of Nx and the hydroxyl group of Tyr-112 strongly influence the site energy of Chl*a* 604 (Müh et al., 2010). This modeling is supported by experiments showing that the conformational changes of Nx influence the Nx-Chl*a* 604-L2 interactions and adjust the triplet energy distribution in LHCII (Zhang et al., 2014). The functions of Nx have not yet been fully understood because of conflicting observation results.

In this study, the structural and functional significance of the unique features of Nx binding have been investigated using different LHCII species, including in vitro reconstituted LHCIIs either containing or lacking Nx, and also using LHCII purified from the wild type (WT-LHCII) and the Nx-lacking mutant *aba4-3* of Arabidopsis (native-LV). We have studied the binding affinity of Nx and its effects on the xanthophyll cycle and the transiently generated NPQ. Our results show that the binding of Nx and Vx to trimeric LHCII is closely coordinated and, thereby, directly affects the operation of the xanthophyll cycle and the dynamics of transiently generated NPQ.

RESULTS

Binding of Vx Is Apparently Competitively Inhibited by Nx Binding

LHCII is a membrane protein complex that can bind photosynthetic pigments in vitro to form recombinant functional complexes with native configuration. This allows for the manipulation of the Car composition and the study of the structure-function relationship of different Cars in the complexes. Table I shows the pigment stoichiometries, determined by HPLC, of recombinant LHCIIs refolded in the presence or absence of Nx. The presence of Nx in the reconstitution process did not change the Chl*a*/*b* ratio of LHCII, which was in the range of 1.11 to 1.18. Since the amount of Chl bound to the recombinant LHCII was 12 for every 2 Lut (Croce et al., 1999), the stoichiometry of the bound Car in LHCII was calculated relative to Chl. LHCII refolded in the presence of all three Cars (Lut, Vx, and Nx: re-LNV) had the normal Car composition: ~1.9 Lut, ~1.2 Nx, and trace amounts of Vx. Omitting Nx in the reconstitution process (re-LV) increased the Vx content to 0.6, indicating that Nx binding was a key factor interfering with the binding of Vx to the LHCII complexes.

This interference was further investigated by Nx reassembly experiments with LHCII complexes lacking Nx, following the procedure described by Hobe et al. (2006). Nx was reassembled into different Nx-deficient LHCII complexes, including the recombinant re-LV without Nx and the LHCII from the Arabidopsis mutant *aba4-3* that lacks Nx, and isolated by Suc gradient centrifugation of detergent-solubilized thylakoid membranes (band 3 in Fig. 1A). The Suc gradient ultracentrifugation of the different LHCII samples, before and after Nx reassembly, showed two bands corresponding to trimeric and monomeric LHCIIs (Fig. 1B). The bands corresponding to the trimeric LHCII were extracted and further characterized. Figure 1C shows the pigment composition of the different complexes. According to our analysis (data not shown), WT-LHCII contains 13 Chl/2 Lut. The amounts of the different Cars were calculated relative to the Chl content, based on the assumption that each monomer binds 13 Chls. This value differs from that of recombinant LHCII, where each monomer was assumed to bind 12 Chls. The Car contents were similar in both LHCII

Downloaded from on October 18, 2017 - Published by www.plantphysiol.org
Copyright © 2017 American Society of Plant Biologists. All rights reserved.

Table I. *Pigment composition of the recombinant LHCII complexes reconstituted with the pigment mixture with or omitting neoxanthin*

The LHCIIs were reconstituted as described before. The Lhcb apoprotein were refolded with pigment mixture with neoxanthin (re-LNV) or omitting neoxanthin (re-LV). tr, Trace; –, not detectable.

Sample	Chl*a*/*b*	Chl	Lut	Nx	trans-Vx
re-LNV	1.11 ± 0.04	12	1.9 ± 0.19	1.2 ± 0.09	tr
re-LV	1.12 ± 0.04	12	2.0 ± 0.11	–	0.6 ± 0.06

species lacking Nx, with 2 Lut and 0.5 Vx bound to native-LV and 2.1 Lut and 0.6 Vx bound to the recombinant ones. Reassembling Nx molecules back to the Nx-lacking LHCII did not alter the Chl or Lut composition of both the recombinant and native LHCIIs. However, the amount of bound Vx decreased significantly upon Nx reassembly. Vx binding in the native-LV decreased from 0.5 to 0, and that in the reconstituted complex decreased from 0.6 to 0.1. Both experiments show clearly that the binding of Nx resulted in a release of Vx from trimeric LHCII.

The interference of Nx on Vx binding was quantified by titrating Nx at concentrations ranging from 5 to 60 μg mL^{-1} into re-LV (Fig. 2). The amount of Lut bound to the complexes did not change significantly over the titration range, while those of bound Nx or Vx showed an inverse relationship, saturating at the Nx concentration of ~40 μg mL^{-1}. To investigate the conformational changes of LHCII during the Nx titration, circular dichroism (CD) spectra were recorded in the visible wavelength range, reflecting the dipole-dipole interactions of the pigments in LHCII (Fig. 2B). WT-LHCII showed the typical CD spectrum of LHCII as reported previously (Hobe et al., 1994). The ratio of the amplitudes of the two negative bands at 491 and 473 nm (CD_{491nm}/CD_{473nm}) was proportional to the amount of Nx bound in the complexes (Croce et al., 1999; Hobe et al., 2006; Liu et al., 2008). Increasing Nx in the reconstitution process resulted in an enhanced CD_{491nm}/CD_{473nm} ratio of the LHCII (Fig. 2B, inset). This demonstrated, first, the authenticity of the reconstituted LHCII and, second, that the amount of Nx determined chromatographically was quantitatively bound to the complexes.

One possible explanation of these results is the competitive binding to the same site. It was demonstrated previously that Vx easily underwent isomerization from all-trans- to cis-configurations (Niedzwiedzki et al., 2005; Grudzinski et al., 2016), which might allow it to occupy the N1 position, as was observed in the parasitic angiosperm *Cuscuta reflexa* (Snyder et al., 2004). To exclude that Vx might isomerize during reconstitution and bind to the N1 position in the absence of Nx, we used resonance Raman spectroscopy that specifically identified 9-cis-isomers by three characteristic bands at 1,134, 1,202, and 1,215 cm^{-1} (Ilioaia et al., 2011; Fig. 3A). The Raman spectrum of LV-LHCII lacked the peaks typical for the 9-cis-isomer, while this is always present in the spectra of re-LN complexes due to the bound Nx. The absence of 9-cis-Vx was verified by HPLC of the reconstituted LHCII: no signal of cis-Vx could be seen (Fig. 3B). Moreover, the second derivative of the absorption spectra of re-LV showed a peak at 486 nm, and that of re-LN showed a peak at 488 nm (Fig. 3C), which refer to the S0 → S2 transition of Vx at the V1 site and that of Nx at the N1 site, respectively. According to the proposal based on previous research (Caffarri et al., 2001) that the red-most S0 → S2 transition of Vx at the V1 site is 485 nm and that at the N1 site is 488 nm, it is obvious that the Vx in re-LV is in an all-trans-configuration and located at the V1 site. All three findings clearly indicated that it was not possible for trans-Vx to bind to the N1 position, because only a cis-Car with a C-5-C-6 epoxide structure fulfills the prerequisite for binding to this site (Phillip et al., 2002).

Apparent Competitive Binding of Nx and Vx to LHCII Results in Changes in Conformation and in the Transition Energy Level of LHCII

Spectroscopic analysis was conducted to investigate the influence of the Nx bound to LHCII on the conformation and transition energies of LHCII (Fig. 4). Figure 4A shows the CD spectra of the different LHCIIs isolated from wild-type Arabidopsis (WT-LHCII) and the *aba4-3* mutant before and after the Nx reassembly [native-LV(Nx)]. WT-LHCII had, in the Qy region, two negative bands: one at 680 nm and the other at 650 nm accompanied by a shoulder at 640 nm; in the Soret region, it had one at 491 nm with a shoulder at 498 nm and the other at 473 nm. Native-LV(Nx) showed a similar spectrum to WT-LHCII, indicating the restoration of the WT-LHCII configuration by inserting Nx back to the native-LV, meanwhile confirming the correct insertion of Nx. Compared with WT-LHCII, native-LV that lacks Nx showed significantly decreased amplitudes of the negative bands at 650 and 491 nm, accompanied by the appearance of a stronger shoulder at 640 and 498 nm (Fig. 4A). The amplitude of the negative band at 473 nm increased enormously. Figure 4B shows the absorption spectra of WT-LHCII, native-LV, and native-LV(Nx). It is clear that lacking Nx in LHCII induced changes in transit energy in the Soret region. Besides, the native-LV minus WT-LHCII absorption difference spectrum in the Qy region also revealed a slight reduction of the absorption around 654 and 678 nm of the LHCII lacking Nx (Fig. 4B, inset). The fluorescence excitation spectra were measured by monitoring the Chl*a* emission (680 nm) over a spectrum

Downloaded from on October 18, 2017 - Published by www.plantphysiol.org
Copyright © 2017 American Society of Plant Biologists. All rights reserved.

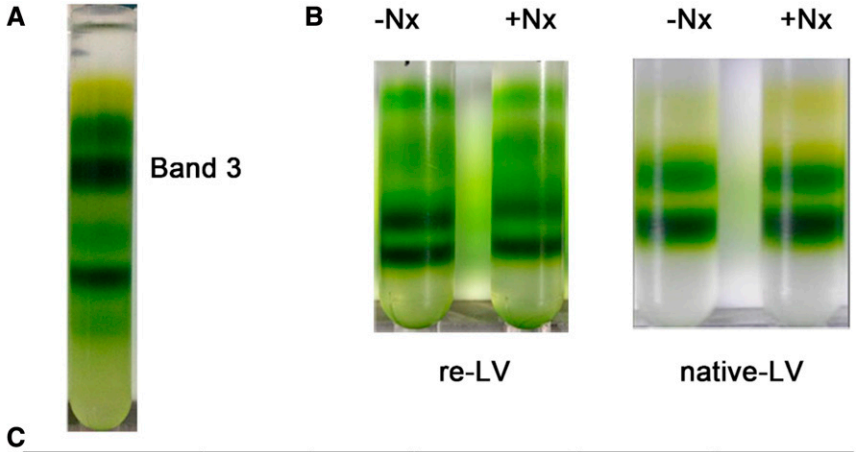

C

sample	Chl *a/b*	Chl	Lut	Nx	*trans*-Vx
WT	1.27	13	1.9 ± 0.04	1.0 ± 0.09	tr
re-LV	1.12	12	2.1 ± 0.12	—	0.6 ± 0.07
re-LV (Nx)	1.11	12	2.1 ± 0.15	1.1 ± 0.05	0.12 ± 0.04
native-LV	1.24	13	2.0 ± 0.09	—	0.5 ± 0.09
native-LV (Nx)	1.20	13	1.9 ± 0.14	1.1 ± 0.05	tr

Figure 1. Nx reassembly experiments with recombinant or isolated native LHCII. A, Suc gradient centrifugation of detergent-solubilized thylakoid membranes. Band 3 is the WT LHCII trimer. B, Suc gradients of LHCIIs after incubation with Nx (+Nx) or without Nx (−Nx) to the reconstituted LV-LHCII (re-LV) or native Nx lacking LHCII isolated from Arabidopsis (native-LV). The Nx reassembly experiments were performed according to the method described by Hobe et al. (2006). The incubations were carried out for 24 h on ice, and then the mixtures were loaded on the Suc gradients. C, Pigment composition of the different LHCII complexes after the reassembly experiments. tr, Trace; WT, wild type; –, not detectable. Data are expressed as means ± SD ($n \geq 3$).

from 350 to 600 nm at room temperature (Fig. 4C). The spectra were normalized in the range of 350 to 390 nm, where the majority energy sensitizing Chl*a* fluorescence emission was from Chl*a*, rather than from Car, or other pigments. The reduction in energy emission around 490 nm implied the lack of energy transfer from Nx to Chl*a* in LHCII.

In conclusion, spectral analysis clearly shows that occupation of the N1 site affected the dipole-dipole interactions of Chls and Cars in the complexes, which, in turn, resulted in changes in the transition energy and, thereby, modulated the energy transfer to Chl*a*.

Binding of Nx Influences the Xanthophyll Cycle Kinetics Directly and the Transiently Generated NPQ

The kinetics of the deepoxidation of Vx in LHCII, with or without Nx, was investigated to elucidate its impact on the xanthophyll cycle. The deepoxidation of Vx in the LHCII was performed at 28°C, catalyzed by a recombinant VDE in the presence of all the cofactors, including monogalactosyldiacylglycerol (MGDG) and ascorbate, according to the method described previously (Morosinotto et al., 2002). The kinetics of the deepoxidation reaction fitted well to a single exponential curve. Conversion of free pigment Vx to Zx was almost completed within 15 min (Fig. 5A; k = 174 [± 17.8] × 10^{-3} min^{-1}). Adding detergent-solubilized Nx to the reaction did not change the deepoxidation rate significantly (Fig. 5B; k = 171 [± 18.4] × 10^{-3} min^{-1}). This result demonstrated that Nx did not interfere with the VDE reaction converting free pigment Vx to Zx. Figure 5C shows the deepoxidation kinetics of re-LV, which reveals two features of the VDE kinetics of LHCII in the absence of Nx. First, the deepoxidation of Vx in LHCII was strongly retarded (k = 10.4 [± 1.5] × 10^{-3} min^{-1}). Second, Vx could still be completely deepoxidized after ~220 min, indicating that all Vx was accessible for VDE in the LHCII without Nx (Fig. 5C). Adding detergent-solubilized Nx to the deepoxidation reaction mixture of re-LV significantly shortened the VDE reaction; all Vx was deepoxidized within 30 min (Fig. 5D). The rate constant was increased 7-fold, from $k = 10.4 \times 10^{-3}$ min^{-1} in the absence of Nx (see above) to $k = 72.3 \times 10^{-3}$ min^{-1} in the presence of Nx.

NPQ formation in the thylakoid membrane, modulated by the xanthophyll cycle, is strongly dependent on the pH difference across the thylakoid membrane, which also is strongly dependent on the light intensity. Measured under nonsaturating light intensity, the time course of NPQ displayed a transiently formed NPQ (qE_{TR}) followed by a relaxation phase, which indicated the processes in the reaction center of PSII (Kalituho et al., 2007). Because the coordination between Nx and Vx binding is closely related to the xanthophyll cycle, which, in turn, modulates the activities of PSII, the qE_{TR} in Arabidopsis leaves with or without Nx was studied. Figure 6 shows the comparison of the qE_{TR} measurements of wild-type Arabidopsis and its mutant, *aba4-3*. The rate of qE_{TR} and the maximal NPQ value in wild-type plants were much higher than those in *aba4-3*. Clearly, lack of Nx reduced the qE_{TR} of the plants. This result seems inconsistent with the observation of

Downloaded from on October 18, 2017 - Published by www.plantphysiol.org
Copyright © 2017 American Society of Plant Biologists. All rights reserved.

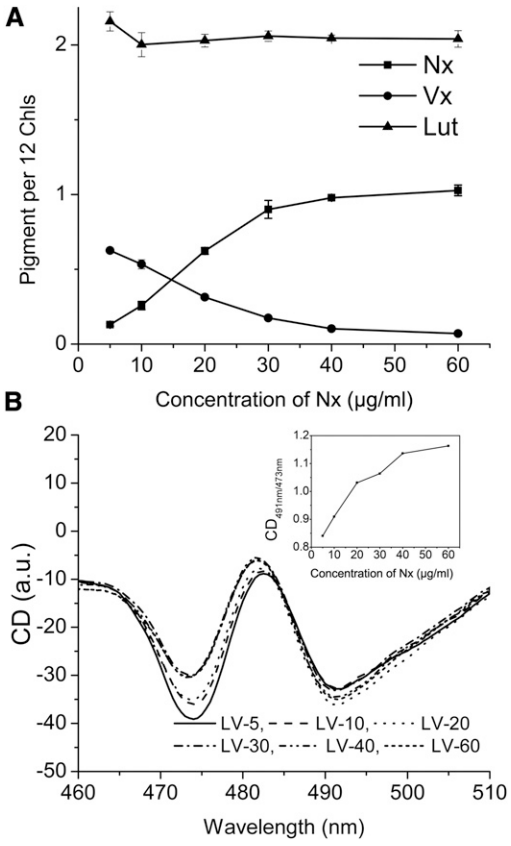

Figure 2. Changes of pigment composition and spectroscopic characterization of different LHCII complexes containing different amounts of Nx. A, Changes of Car composition during the Nx titration experiment using re-LV. The Car composition was calculated based on the assumption that each monomer binds 12 Chls. Data are expressed as means ± SD ($n = 3$). B, CD spectra of LHCII containing different amounts of Nx during the Nx titration experiment. Nx concentrations ranged from 5 to 60 μg mL^{-1}. The inset shows the changes of the ratio of the two CD bands at 491 and 473 nm (CD_{491nm}/CD_{473nm}) along with the increment of Nx concentrations in the reassembly reaction. a.u., Arbitrary unit.

Dall'Osto et al. (2007), who could not detect any difference in the NPQ value of wild-type and *aba4-1* lines. Possibly, the NPQ they measured was a steady-state NPQ rather than the qE_{TR}, which reflects the physiological status of PSII more clearly.

DISCUSSION

The above experiments show that Nx binding to LHCII complexes adversely affects Vx binding, accelerates the first reaction of the xanthophyll cycle, namely, Vx deepoxidation, and promotes the induction of the transient NPQ. Nx is a key Car in the chloroplasts of oxygenic phototrophs, which is only found at the monomer-monomer interface of LHCII and at the interface of LHCII, CP26, and CP29 in PSII. It is always hydrogen bonded to the luminal-loop residue, Trp-112, and closely interacts with Chl*b* (Takaichi and Mirauro, 1998; Caffarri et al., 2007). Studies on the physiological roles of Nx reveal that Nx is important for scavenging superoxide anions at PSII (Dall'Osto et al., 2007), for quenching Chl triplet excitation in LHCII (Zhang et al., 2014), and also for regulating energy-use efficiencies in PSII (Ruban et al., 2007).

In this study, the amounts of bound Cars of monomeric LHCII were measured and calculated assuming that each recombinant monomer binds 12 Chls and that native monomeric LHCII contains 13 Chls. These assumptions were based on our HPLC measurements of Chl contents of re-LHCII and native-LHCII and calculated according to the method discussed (Yang

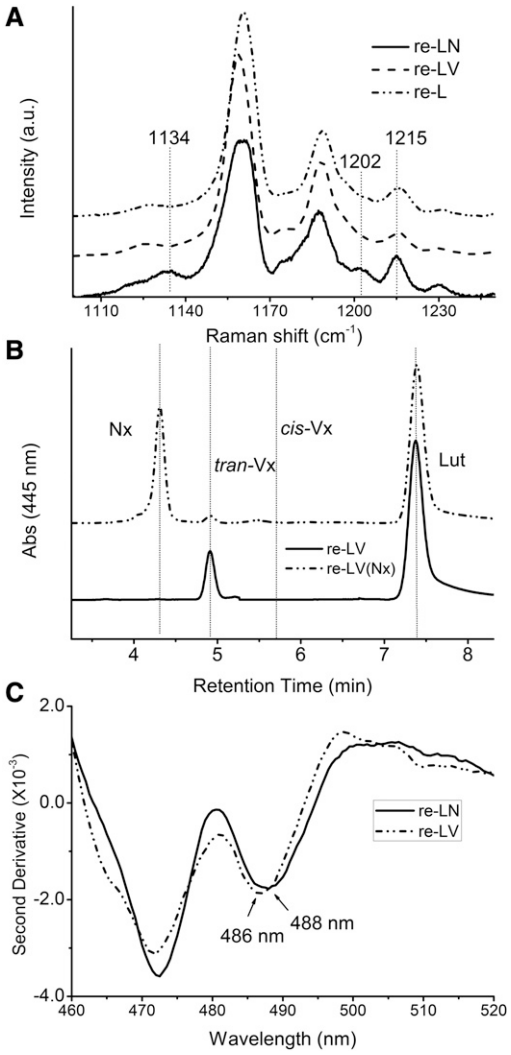

Figure 3. Configuration of violaxanthin in LHCII. A, Raman spectra of LHCII reconstituted with different Car compositions. B, HPLC measurements of Nx lacking LHCII before or after Nx reassembly. The known retention time of cis-Vx is indicated by a simple vertical line. C, Second derivative of the absorption spectra in the Soret region of the LHCII containing different Cars. re-L, LHCII containing only Lut; re-LN, LHCII containing only Lut and Nx; re-LV, LHCII containing only Lut and Vx; re-LV(Nx), LHCII containing all three Cars (Nx was reassembled back to re-LV).

Downloaded from on October 18, 2017 - Published by www.plantphysiol.org
Copyright © 2017 American Society of Plant Biologists. All rights reserved.

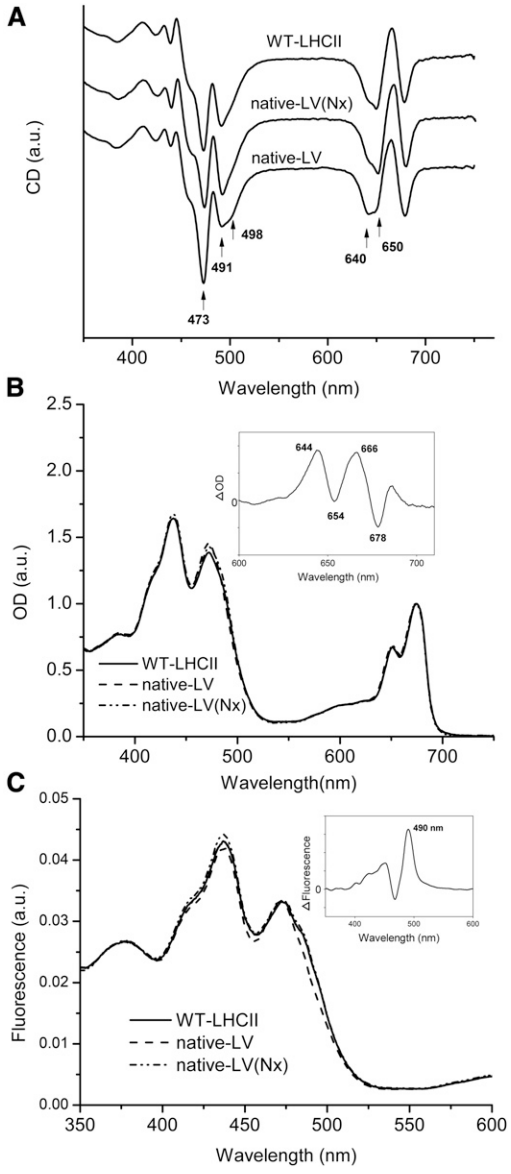

Figure 4. Spectroscopic characteristics of different LHCII species. A, CD spectra of WT-LHCII and native-LV before or after Nx reassembly. The CD spectra were normalized to A_{675}. B, Room-temperature absorption spectra of WT-LHCII and native-LV before or after Nx reassembly. The spectra were normalized at the maximal absorption in the Qy region. The inset shows the native-LV minus WT-LCHII difference spectrum. C, Room-temperature fluorescence excitation spectra of WT-LHCII and native-LV before or after Nx reassembly. The fluorescence emission spectra were measured by monitoring the Chl*a* fluorescence emission at 680 nm. The spectra were normalized in the region between 350 and 390 nm, where the majority fluorescence emission was sensitized by Chl*a* rather than by other pigments. The inset shows the WT-LHCII minus native-LV difference absorption spectrum.

et al., 1999; Liu et al., 2008). The nonconformity of our measured Chl amounts in the native-LHCII monomer (13 Chls) with those of LHCII in the crystal structure (14 Chls) might be attributed to the loss of one or two peripherally bound Chls during the purification process. Because both the Chl*a/b* and Chl/Lut ratios of all the samples did not change significantly, it is justified to discuss only the relationship of Vx and Nx in our study. Our results show that Nx is very important both in operating the xanthophyll cycle and in inducing the transiently generated NPQ of oxygenic photosynthesis via its adverse effect on the Vx binding to LHCII.

Binding of Nx at the N1 Site and Vx at the V1 Site in LHCII Trimer Are Closely Coordinated

Our study shows that Nx not only contributes to the structural stability of the pigment protein complexes but also fulfills various physiological functions. Previous in vitro reconstitution experiments have demonstrated that LHCII has a very high affinity for Nx at the N1 site compared with that for Vx at the V1 site: LHCII binds quantitatively one Nx per monomer even when reconstituted with pigments at a high Vx/Nx ratio (Hobe et al., 2006). This feature also was proven in an Arabidopsis mutant overexpressing β-carotene hydroxylase, where the Nx binding was not affected even though the Vx content was increased 2-fold (Davison et al., 2002). In this study, the binding of Nx and Vx was shown to be closely coordinated in trimeric LHCII complexes. The two LHCII species lacking Nx, either that reconstituted in vitro or the native LHCII isolated from *aba4-3*, bind more than half a Vx per monomer. Upon the reassembly of Nx in LHCII, Vx is dissociated from LHCII, with a quantitatively negative correlation to the amount of Nx binding in the complexes (Table I; Figs. 1–3). The reassembly of Nx to LHCII has not only confirmed the previous observation that the binding of Nx to LHCII is fully reversible (Hobe et al., 2006) but also reveals, to our knowledge for the first time, the corresponding reversible dissociation of Vx of the adjacent monomer (Fig. 1). Structural analysis shows that the observed competitive relationship between Nx and Vx binding to LHCII should be attributed to the coordination of the two binding N1 and V1 sites rather than to the competition for the N1 site. Raman spectrum and HPLC data have excluded the possibility of 9-cis-carotenoid binding to the N1 site, since no 9-cis-5,6-epoxy structure was detected; furthermore, previous studies have revealed that the binding at the N1 site is highly specific for Cars with a 9-cis-5,6-epoxy structure (Bungard et al., 1999; Phillip et al., 2002). The second derivative of the absorption spectrum of re-LV (Fig. 3C) confirmed that Vx was located at the V1 site, rather than at the N1 site, because it showed only the specific absorption peak (485.5 nm) of Vx at the V1 site (Caffarri et al., 2001).

The high-resolution structure of LHCII (Liu et al., 2004; Standfuss et al., 2005) has shown that Nx is stabilized in LHCII by a hydrogen bond with Tyr-112 and hydrophobic interactions with five surrounding Chl*b* molecules, which are very close to the interface of the two adjacent monomers where the phosphatidylglycerol (PG), Vx, and several Chls form extensive hydrophobic interactions. The Nx of one monomer interacts indirectly, via the intervening pigment cluster Chl*b* 606-607,

Downloaded from on October 18, 2017 - Published by www.plantphysiol.org
Copyright © 2017 American Society of Plant Biologists. All rights reserved.

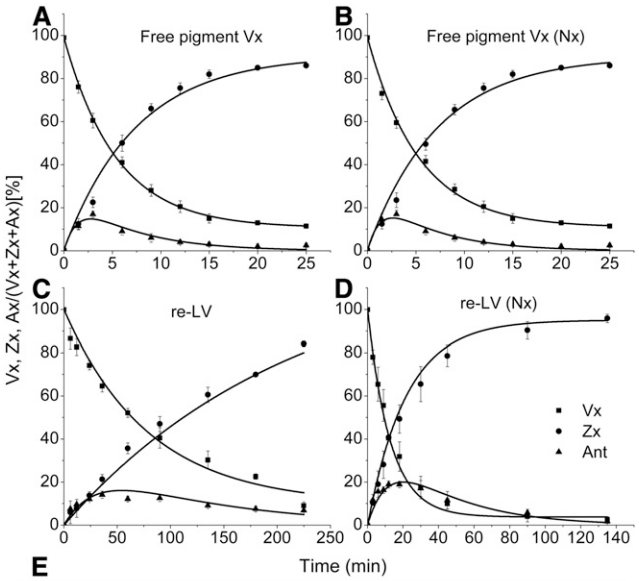

E

Rate constant (10^{-3} min^{-1})	Free pigment Vx	Free pigment Vx (Nx)	re-LV	re-LV (Nx)
k	174 ± 17.8	171 ± 18.4	10.4 ± 1.5	72.3 ± 11.0

Figure 5. Time course of the in vitro Vx deepoxidation reaction in the LHCII trimer. The VDE was overexpressed in *E. coli*. The deepoxidation reaction was performed at 28°C in the presence of MGDG. The VDE content and Vx concentration were in a similar range in all experiments. A, Free pigment Vx deepoxidation. B, Addition of Nx to the reaction system of the free pigment Vx deepoxidation. C, Vx deepoxidation of the re-LV. D, Vx deepoxidation of re-LV after Nx reassembly. E, Rate constants derived for the first step of deepoxidation (Vx → Ant) assuming a first-order kinetics for the reaction. For all reactions, data points were fitted with a single exponential (*k*). Rate constants represent mean values ± SD (n = 3–5). Ant and Ax, Antheraxanthin.

with the Vx of the adjacent monomer, thus providing a plausible explanation for the coordinated binding relationship of the two different Cars in LHCII at the monomer-monomer interface. The V1 site is empty in LHCII lacking the first eight N-terminal residues (4LCZ; Wan et al., 2014). Figure 7A shows a comparison of the monomer-monomer interactions of the full-length and N-terminally truncated LHCII structures by superimposing the two x-ray structures (1RWT on 4LCZ). The red circles indicate regions where the two structures differ significantly, located mainly at or near the Vx pocket (Liu et al., 2004; Wan et al., 2014). In the structure of 1RWT, the cyclohexane epoxide head of Vx pointing to the stroma side is hydrogen bonded to PG, and the other head, located at the luminal side, is fixed by a cleft formed with the carboxyl group of the 17-propionic acid side chain of Chl*b* 607 and the C-terminal residues, especially Trp-222 and Ala-225 (Fig. 7B). In the absence of Vx (4LCZ), the propionyloxy group of Chl*b* 607 moves 1.69 Å forward toward the empty hole of the V1 site (Wan et al., 2014). Comparing the two structures (1RWT and 4LCZ) reveals that the distance of Chl*b* 607, which interacts closely with Chl*b* 606 and Gln-131 (Liguori et al., 2015), to the V1 site changes from 2.91 to 1.22 Å, depending on whether the V1 position is occupied or not. Therefore, it is possible that the van der Waals repulsion between Chl*b* 607 and Vx influences the binding strength of Vx to the V1 site. Considering that Nx is located in the same region, interacting with Chl*b* 606-607 (Liu et al., 2004), it is reasonable to suppose that the absence of Nx in the cleft region releases the steric hindrance and increases the binding strength of Vx. Therefore, we conclude that the binding of Nx is coordinated closely with that of the Vx of the adjacent monomer in the trimer by controlling the affinity of the V1 site. This conclusion is supported by previous observations showing that Vx is more tightly bound to monomeric than to trimeric LHCII because there is no monomer-monomer interface interaction and, therefore, no steric hindrance to the V1 site caused by occupation of the N1 site by Nx (Ruban et al., 1999).

According to the site energy calculation by Müh et al. (2010), the absorption around 650 nm can be attributed mainly to Chl*b* 606-607, which interacts hydrophobically with Nx. The close interaction between Nx and Chl*b* 606-607 also is supported by the spectroscopic analysis of the native-LHCII with or without Nx. In comparison with LHCII isolated from wild-type Arabidopsis, the LHCII isolated from *aba4-3* showed reduced absorption at 654 nm and increased absorption at 644 nm, which agrees with earlier results (Fuciman et al., 2012; Fig. 4B, inset). This coincides with the reduced amplitude of the 650-nm peak in the CD spectrum. These data indicate that the loss of Nx in the Nx-Chl*b* region results in an distinct change in the conformation of Chl*b* 606-607, which induces the variations in both its transition energy and the dipole-dipole interaction with other pigments: the same changes are observed in response to the presence and

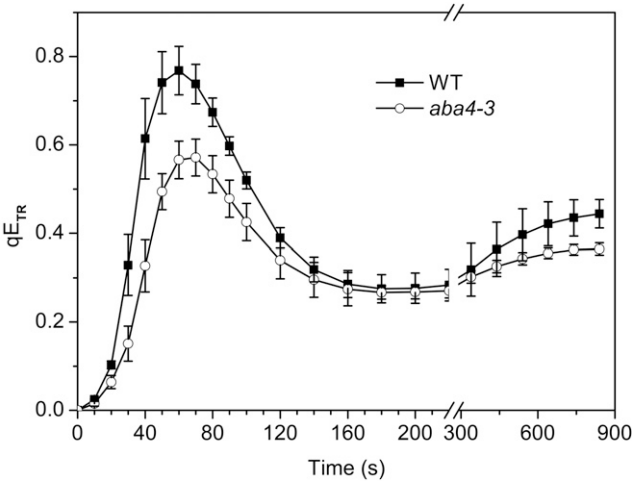

Figure 6. qE_{TR} in wild-type (WT) Arabidopsis and its mutant *aba4-3*. The dynamics of qE_{TR} were determined in dark-adapted wild-type Arabidopsis and its mutant *aba4-3*. Leaves were illuminated for 14 min at a light intensity of 50 μmol photons m^{-2} s^{-1}, followed by 10 min of dark incubation. Mean values ± SD of three to four independent experiments are shown.

Downloaded from on October 18, 2017 - Published by www.plantphysiol.org
Copyright © 2017 American Society of Plant Biologists. All rights reserved.

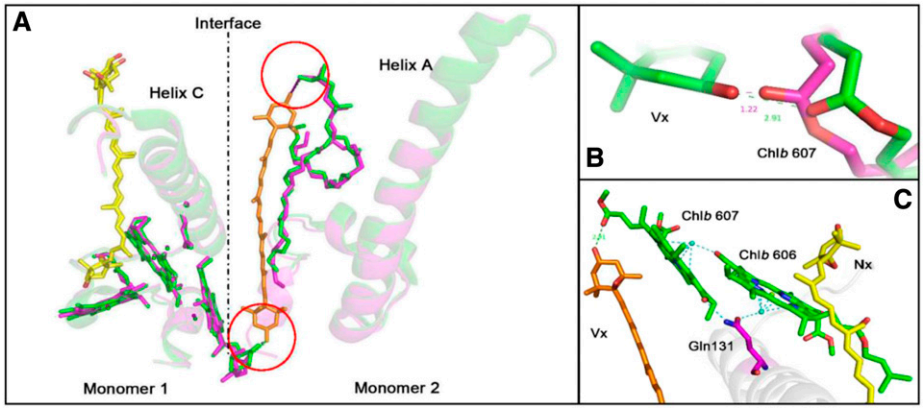

Figure 7. Representation of the Vx-binding site in LHCII. A, The interface of adjacent monomers. Green, 1RWT; purple, 4LCZ. B, The interaction of one cyclohexane epoxide head of Vx and Chl*b* 607. Green, 1RWT; purple, 4LCZ. C, The interaction of Vx and Nx between adjacent monomers in 1RWT.

absence of Nx in the Nx reassembly experiment. Considered together, these results support the hypothesis that the interaction between Nx and the Chl*b* 606-607 cluster plays important roles in modulating the function of LHCII.

Phylogenetically, the appearance of Nx in the chloroplast is associated with the appearance of Chl*b* (Takaichi and Mirauro, 1998). The distribution of Nx is confined to the antenna proteins of PSII, namely, to LHCII, CP26, and CP29 (Takaichi and Mirauro, 1998; Caffarri et al., 2007). The structural analysis of LHCII and CP29 shows that Nx is located in contact distance to Chl*b* with hydrophobic interactions (Liu et al., 2004; Standfuss et al., 2005; Pan et al., 2011). More recently, it has been shown that Nx, with its cyclohexane ring stretching out of the antenna protein complexes into the exterior membrane region, is located mainly between different antenna proteins of PSII and dominates the intermolecular interactions between LHCII-CP29 and LHCII-CP26 (Wei et al., 2016). The key role of Nx is emphasized further by the close relationship, shown in this article, between the N1 and V1 sites.

The Interaction between Nx and Vx Is Very Important for Regulating the Xanthophyll Cycle

One of the possible physiological functions of these structural modulations by Nx is its influence on the xanthophyll cycle that we have demonstrated. The xanthophyll cycle is an important process in photoprotection (Eskling et al., 1997). When too many protons are accumulated in the lumen under strong light conditions, photosynthesis triggers Vx deepoxidation catalyzed by VDE, a water-soluble enzyme located on the luminal side of thylakoids (Hager, 1969). The high-light stress causes LHCII aggregation and MGDG cluster formation at the luminal face of the thylakoid membrane, which may constitute a signal activating the mechanisms of Vx dissociation and its migration in the thylakoid membrane to VDE (Macko et al., 2002; Schaller et al., 2010). This would locate the deepoxidation in the MGDG-enriched membrane region and the release of Vx into the lipid phase (Yamamoto and Higashi, 1978; Jahns et al., 2009). Vx can bind to all Car-binding sites in LHCII except the N1 site, where a 9-cis-Car with 5,6-epoxy structure is required (Croce et al., 1999; Snyder et al., 2004). Although Vx deepoxidation is possible for the Vx bound to almost all sites (Jahns et al., 2001; Wehner et al., 2004, 2006), the peripherally located loosely bound Vx, which exists only in the LHCII complexes, has the highest VDE reaction rates (Ruban et al., 1999; Duffy and Ruban, 2012; Xu et al., 2015; Grudzinski et al., 2016). All these data support the hypothesis that LHCII is the main pool for VDE and that the dissociation of Vx from LHCII and its migration to the lipid matrix are the limiting factors regulating the xanthophyll cycle.

Our data also provide a structural basis of the Vx dissociation mechanism. The in vitro deepoxidation experiments of the LHCII-bound Vx show that the reverse-correlated binding of Vx and Nx in LHCII plays key roles in modulating the dissociation of Vx from LHCII. The deepoxidation rate of the LHCII trimer without Nx is reduced by a factor of 7, compared with complexes incubated with Nx (Fig. 5). This is consistent with the demonstration in vivo that the Arabidopsis *aba4-1* mutant showed a much slower increase of the deepoxidation index than the wild-type plants (Dall'Osto et al., 2007). The fact that Nx influences only the deepoxidation rate of LHCII-bound Vx, but not that of the free pigment, strongly suggests that the effect of Nx on Vx deepoxidation is related to the substrate released from LHCII rather than to the kinetics of the deepoxidation. This observation reveals an important function of the LHCII-bound Nx in modulating the xanthophyll cycle and, thus, also the explanation of the mechanism for regulating Vx release from LHCII to the VDE reaction site. Furthermore, the delayed deepoxidation in the LHCII of the Arabidopsis mutant *aba4-3* observed in vitro (Fig. 5) is accompanied by its effect on the qE_{TR} measured with the plant leaves in vivo (Fig. 6). Lack of Nx binding in LHCII retarded the deepoxidation and, concomitantly, reduced the qE_{TR} of excitation energy in leaves. Our observation is in agreement with that of Kalituho et al. (2007), who observed a much reduced qE_{TR} in the Zx-deficient *npq1*

Downloaded from on October 18, 2017 - Published by www.plantphysiol.org
Copyright © 2017 American Society of Plant Biologists. All rights reserved.

mutant and an increased qE_{TR} in the Zx-rich *npq2* mutant. Further research has found that the VDE rate is the rate-limiting factor controlling the kinetics of NPQ (Johnson et al., 2008; Chen and Gallie, 2012). Here, we show that it is the coordination between Nx and Vx binding that plays important roles in modulating the VDE activity that regulates the transiently generated NPQ.

CONCLUSION

Nx is the only form of neoxanthin existing in the photosynthetic apparatus. It has been found that the binding of Nx to LHCII is coordinated by Chl*b* and near Vx at the interface of different LHCII monomers. The presence of Nx repels Vx from the V1 site of the adjacent monomer. The coordination of Nx and Vx is of great significance in regulating the xanthophyll cycle as well as in regulating the dynamics of NPQ in plants.

MATERIALS AND METHODS

Plant Material and Preparation of Native LHCII

The Arabidopsis (*Arabidopsis thaliana*, ecotype Columbia) T-DNA insertion line *aba4-3* (SALK_137455C) was obtained from the European Arabidopsis Stock Centre (http://arabidopsis.info) and verified by PCR. The wild-type Arabidopsis and its mutant *aba4-3* were grown for 5 weeks in a growth chamber with a regime of 8 h of light (100 μmol photons m^{-2} s^{-1}) and 16 h of dark at 22°C and 50% to 70% relative humidity. Thylakoid membranes, isolated from leaves of different *Arabidopsis* species by the method of Zhang et al. (1999), were ultracentrifuged on a Suc gradient (0.1–1 M Suc, containing 0.06% *n*-dodecyl-α-D-maltoside and 10 mM HEPES, pH 7.5). The band corresponding to the native LHCII trimers was extracted for experiments.

Preparation of Recombinant LHCII

The Lhcb1 apoproteins, overexpressed and purified from *Escherichia coli*, were reconstituted with different thylakoid pigments (Chl*a*/*b* = 2, Car composition varied according to needs) as described previously (Liu et al., 2008). The LHCII trimerization was performed in an Ni-chelating Sepharose fast-flow column (Amersham Biosciences; column, 0.8 cm × 4 cm [Bio-Rad]) according to the method of Rogl et al. (1998). The LHCII trimers were purified by an 18-h ultracentrifugation (200,000*g* at 4°C) on Suc density gradients (0.1–1 M Suc, containing 0.1% *n*-dodecyl-β-D-maltoside and 5 mM phosphate buffer, pH 7.5).

Nx Insertion Reaction

Nx reassembly to the in vitro reconstituted LHCII was started at the last step of trimerization. The Nx for the insertion reaction, solubilized in 50 μL of ethanol, was mixed with the elution buffer (0.05% [w/v] Triton X-100, 0.1 mg mL^{-1} PG, 100 mM Tricine-HCl, and 150 mM imidazole, pH 7.5). After passing through 0.22-μm sterile filters, the Nx concentration in the elution buffer was adjusted to 50 μg mL^{-1}. The samples were eluted by the Nx solution from the Ni-chelating Sepharose column and incubated on ice for 24 h, then underwent the same ultracentrifugation process as the recombinant LHCII. The bands corresponding to the trimers were collected.

Inserting Nx into the native LHCII was performed by the modified method of Hobe et al. (2006). The native LHCIIs were first concentrated ~20-fold on 30-kD Centricon devices, then adjusted to the same Chl concentration, and finally diluted 10-fold with the same elution buffer containing Nx as described previously for the reconstituted LHCII. Subsequently, the mixtures were incubated for 24 h on ice and then ultracentrifuged, as was done for the reconstituted LHCII. The bands corresponding to the trimers were collected for further analysis.

Pigment Analysis

The pigments of LHCII isolated by Suc gradient ultracentrifugation were extracted with 2-butyl alcohol. The pigment composition was analyzed with an RP-C18 column (Grace) equipped for HPLC (Waters) as described (Qin et al., 2015).

Spectroscopic Analyses

The room-temperature absorption spectra were recorded using a Shimadzu UV-VIS 2550 spectrophotometer, and the fluorescence excitation spectra were recorded by monitoring Chl*a* fluorescence emission at room temperature using a Hitachi F-7000 spectrofluorometer. The excitation spectra were normalized in the region between 350 and 390 nm because, in this region, most of the energy sensitizing the Chl*a* fluorescence emission came from Chl*a* rather than from Car or other pigments.

CD spectra from 350 to 750 nm were recorded with a Chirascan apparatus (Applied Photophysics) at 4°C, with the spectral bandwidth set to 2 nm and a step size of 0.5 nm.

Resonance Raman spectra were measured using a JY-T64000 (Horiba/Jobin Yvon) Raman spectrophotometer. The sample holder was cooled by liquid nitrogen with a TMS 94 temperature controller (Linkam Scientific Instruments). The excitation wavelength was set to 488 nm.

In Vitro Deepoxidation

The VDE enzyme was expressed in *E. coli* strain Rosetta-gamin B (DE3), collected, and purified by the method of Gao et al. (2013). In vitro deepoxidation was conducted with the method reported previously (Morosinotto et al., 2002) with some modifications. LHCII (3 μg of Chl) was mixed with 60 μg mL^{-1} MGDG and added to the reaction buffer (100 mM citrate buffer and 0.03% *n*-dodecyl-β-D-maltoside) and ~1.5×10^{-3} units of the VDE enzyme preparation. For kinetic analysis, the reaction was stopped by mixing the sample with 2-butanol at different time intervals. The pigment stoichiometry was analyzed as described before.

Transiently Generated NPQ of Excitation Energy

To measure the dynamics of the transiently generated qE_{TR}, dark-adapted wild-type and *aba4-3* mutant plants grown under the same conditions were illuminated for 14 min at the light intensity of 50 μmol photons m^{-2} s^{-1}, followed by 10 min of dark relaxation. The time courses of nonphotochemical fluorescence quenching were recorded over the time span 1 to 900 s. The minimum fluorescence intensity was measured under a weak measuring light (wavelength of 650 nm, 0.5 μmol photons m^{-2} s^{-1}). The maximum fluorescence in the dark-adapted state (F_m) and during illumination with actinic light (F_m') were measured by applying a saturating pulse of white light (4,500 μmol photons m^{-2} s^{-1} for 0.8 s). The qE_{TR} was calculated as $(F_m - F_m')/F_m'$.

ACKNOWLEDGMENTS

We thank Hugo Scheer (Ludwig-Maximillian University), Jean-David Rochaix (University of Geneva), and Robert J. Porra (Commonwealth Scientific and Industrial Research Organization Plant Industry) for valuable suggestions and critically reading the article; Zhongzhou Chen (China Agricultural University) for suggestions in crystal structure analysis; and Yulong Liu (Institute of Physics, China Agricultural University) for help in resonance Raman spectroscopy.

Received March 6, 2017; accepted March 16, 2017; published March 20, 2017.

LITERATURE CITED

Bungard RA, Ruban AV, Hibberd JM, Press MC, Horton P, Scholes JD (1999) Unusual carotenoid composition and a new type of xanthophyll cycle in plants. Proc Natl Acad Sci USA **96:** 1135–1139

Caffarri S, Croce R, Breton J, Bassi R (2001) The major antenna complex of photosystem II has a xanthophyll binding site not involved in light harvesting. J Biol Chem **276:** 35924–35933

Downloaded from on October 18, 2017 - Published by www.plantphysiol.org
Copyright © 2017 American Society of Plant Biologists. All rights reserved.

Caffarri S, Passarini F, Bassi R, Croce R (2007) A specific binding site for neoxanthin in the monomeric antenna proteins CP26 and CP29 of photosystem II. FEBS Lett **581:** 4704–4710

Chen Z, Gallie DR (2012) Violaxanthin de-epoxidase is rate-limiting for non-photochemical quenching under subsaturating light or during chilling in Arabidopsis. Plant Physiol Biochem **58:** 66–82

Croce R, Weiss S, Bassi R (1999) Carotenoid-binding sites of the major light-harvesting complex II of higher plants. J Biol Chem **274:** 29613–29623

Dall'Osto L, Cazzaniga S, North H, Marion-Poll A, Bassi R (2007) The *Arabidopsis aba4-1* mutant reveals a specific function for neoxanthin in protection against photooxidative stress. Plant Cell **19:** 1048–1064

Davison PA, Hunter CN, Horton P (2002) Overexpression of beta-carotene hydroxylase enhances stress tolerance in Arabidopsis. Nature **418:** 203–206

Duffy CD, Ruban AV (2012) A theoretical investigation of xanthophyll-protein hydrogen bonding in the photosystem II antenna. J Phys Chem B **116:** 4310–4318

Eskling M, Arvidsson PO, Åkerlund HE (1997) The xanthophyll cycle, its regulation and components. Physiol Plant **100:** 806–816

Fehr N, Dietz C, Polyhach Y, von Hagens T, Jeschke G, Paulsen H (2015) Modeling of the N-terminal section and the lumenal loop of trimeric light harvesting complex II (LHCII) by using EPR. J Biol Chem **290:** 26007–26020

Fuciman M, Enriquez MM, Polívka T, Dall'Osto L, Bassi R, Frank HA (2012) Role of xanthophylls in light harvesting in green plants: a spectroscopic investigation of mutant LHCII and Lhcb pigment-protein complexes. J Phys Chem B **116:** 3834–3849

Gao Z, Liu Q, Zheng B, Chen Y (2013) Molecular characterization and primary functional analysis of PeVDE, a violaxanthin de-epoxidase gene from bamboo (Phyllostachys edulis). Plant Cell Rep **32:** 1381–1391

Grudzinski W, Janik E, Bednarska J, Welc R, Zubik M, Sowinski K, Luchowski R, Gruszecki WI (2016) Light-driven reconfiguration of a xanthophyll violaxanthin in the photosynthetic pigment-protein complex LHCII: a resonance Raman study. J Phys Chem B **120:** 4373–4382

Hager A (1969) Light dependent decrease of the pH-value in a chloroplast compartment causing the enzymatic interconversion of violaxanthin to zeaxanthin: relations to photophosphorylation. [in German] Planta **89:** 224–243

Hobe S, Prytulla S, Kühlbrandt W, Paulsen H (1994) Trimerization and crystallization of reconstituted light-harvesting chlorophyll a/b complex. EMBO J **13:** 3423–3429

Hobe S, Trostmann I, Raunser S, Paulsen H (2006) Assembly of the major light-harvesting chlorophyll-a/b complex: thermodynamics and kinetics of neoxanthin binding. J Biol Chem **281:** 25156–25166

Holt NE, Zigmantas D, Valkunas L, Li XP, Niyogi KK, Fleming GR (2005) Carotenoid cation formation and the regulation of photosynthetic light harvesting. Science **307:** 433–436

Ilioaia C, Johnson MP, Horton P, Ruban AV (2008) Induction of efficient energy dissipation in the isolated light-harvesting complex of photosystem II in the absence of protein aggregation. J Biol Chem **283:** 29505–29512

Ilioaia C, Johnson MP, Liao PN, Pascal AA, van Grondelle R, Walla PJ, Ruban AV, Robert B (2011) Photoprotection in plants involves a change in lutein 1 binding domain in the major light-harvesting complex of photosystem II. J Biol Chem **286:** 27247–27254

Jahns P, Latowski D, Strzalka K (2009) Mechanism and regulation of the violaxanthin cycle: the role of antenna proteins and membrane lipids. Biochim Biophys Acta **1787:** 3–14

Jahns P, Wehner A, Paulsen H, Hobe S (2001) De-epoxidation of violaxanthin after reconstitution into different carotenoid binding sites of light-harvesting complex II. J Biol Chem **276:** 22154–22159

Johnson MP, Davison PA, Ruban AV, Horton P (2008) The xanthophyll cycle pool size controls the kinetics of non-photochemical quenching in Arabidopsis thaliana. FEBS Lett **582:** 262–266

Kalituho L, Beran KC, Jahns P (2007) The transiently generated non-photochemical quenching of excitation energy in Arabidopsis leaves is modulated by zeaxanthin. Plant Physiol **143:** 1861–1870

Kirilovsky D (2015) Photosynthesis: dissipating energy by carotenoids. Nat Chem Biol **11:** 242–243

Liguori N, Periole X, Marrink SJ, Croce R (2015) From light-harvesting to photoprotection: structural basis of the dynamic switch of the major antenna complex of plants (LHCII). Sci Rep **5:** 15661

Liu C, Zhang Y, Cao D, He Y, Kuang T, Yang C (2008) Structural and functional analysis of the antiparallel strands in the lumenal loop of the major light-harvesting chlorophyll a/b complex of photosystem II (LHCIIb) by site-directed mutagenesis. J Biol Chem **283:** 487–495

Liu Z, Yan H, Wang K, Kuang T, Zhang J, Gui L, An X, Chang W (2004) Crystal structure of spinach major light-harvesting complex at 2.72 A resolution. Nature **428:** 287–292

Macko S, Wehner A, Jahns P (2002) Comparison of violaxanthin de-epoxidation from the stroma and lumen sides of isolated thylakoid membranes from Arabidopsis: implications for the mechanism of de-epoxidation. Planta **216:** 309–314

Morosinotto T, Baronio R, Bassi R (2002) Dynamics of chromophore binding to Lhc proteins in vivo and in vitro during operation of the xanthophyll cycle. J Biol Chem **277:** 36913–36920

Mozzo M, Dall'Osto L, Hienerwadel R, Bassi R, Croce R (2008) Photoprotection in the antenna complexes of photosystem II: role of individual xanthophylls in chlorophyll triplet quenching. J Biol Chem **283:** 6184–6192

Müh F, Madjet MA, Renger T (2010) Structure-based identification of energy sinks in plant light-harvesting complex II. J Phys Chem B **114:** 13517–13535

Niedzwiedzki D, Krupa Z, Gruszecki WI (2005) Temperature-induced isomerization of violaxanthin in organic solvents and in light-harvesting complex II. J Photochem Photobiol B **78:** 109–114

Oritani T, Kiyota H (2003) Biosynthesis and metabolism of abscisic acid and related compounds. Nat Prod Rep **20:** 414–425

Pan X, Li M, Wan T, Wang L, Jia C, Hou Z, Zhao X, Zhang J, Chang W (2011) Structural insights into energy regulation of light-harvesting complex CP29 from spinach. Nat Struct Mol Biol **18:** 309–315

Phillip D, Hobe S, Paulsen H, Molnar P, Hashimoto H, Young AJ (2002) The binding of xanthophylls to the bulk light-harvesting complex of photosystem II of higher plants: a specific requirement for carotenoids with a 3-hydroxy-beta-end group. J Biol Chem **277:** 25160–25169

Qin X, Suga M, Kuang T, Shen JR (2015) Structural basis for energy transfer pathways in the plant PSI-LHCI supercomplex. Science **348:** 989–995

Rogl H, Kosemund K, Kühlbrandt W, Collinson I (1998) Refolding of Escherichia coli produced membrane protein inclusion bodies immobilised by nickel chelating chromatography. FEBS Lett **432:** 21–26

Ruban AV (2015) Evolution under the sun: optimizing light harvesting in photosynthesis. J Exp Bot **66:** 7–23

Ruban AV, Berera R, Ilioaia C, van Stokkum IH, Kennis JT, Pascal AA, van Amerongen H, Robert B, Horton P, van Grondelle R (2007) Identification of a mechanism of photoprotective energy dissipation in higher plants. Nature **450:** 575–578

Ruban AV, Lee PJ, Wentworth M, Young AJ, Horton P (1999) Determination of the stoichiometry and strength of binding of xanthophylls to the photosystem II light harvesting complexes. J Biol Chem **274:** 10458–10465

Schaller S, Latowski D, Jemioła-Rzemińska M, Wilhelm C, Strzałka K, Goss R (2010) The main thylakoid membrane lipid monogalactosyldiacylglycerol (MGDG) promotes the de-epoxidation of violaxanthin associated with the light-harvesting complex of photosystem II (LHCII). Biochim Biophys Acta **1797:** 414–424

Snyder AM, Clark BM, Robert B, Ruban AV, Bungard RA (2004) Carotenoid specificity of light-harvesting complex II binding sites: occurrence of 9-cis-violaxanthin in the neoxanthin-binding site in the parasitic angiosperm Cuscuta reflexa. J Biol Chem **279:** 5162–5168

Standfuss J, Terwisscha van Scheltinga AC, Lamborghini M, Kühlbrandt W (2005) Mechanisms of photoprotection and nonphotochemical quenching in pea light-harvesting complex at 2.5 A resolution. EMBO J **24:** 919–928

Takaichi S, Mirauro M (1998) Distribution and geometric isomerism of neoxanthin in oxygenic phototrophs: 9′-cis, a sole molecular form. Plant Cell Physiol **39:** 968–977

Downloaded from on October 18, 2017 - Published by www.plantphysiol.org
Copyright © 2017 American Society of Plant Biologists. All rights reserved.

Wan T, Li M, Zhao X, Zhang J, Liu Z, Chang W (2014) Crystal structure of a multilayer packed major light-harvesting complex: implications for grana stacking in higher plants. Mol Plant **7:** 916–919

Wehner A, Grasses T, Jahns P (2006) De-epoxidation of violaxanthin in the minor antenna proteins of photosystem II, LHCB4, LHCB5, and LHCB6. J Biol Chem **281:** 21924–21933

Wehner A, Storf S, Jahns P, Schmid VH (2004) De-epoxidation of violaxanthin in light-harvesting complex I proteins. J Biol Chem **279:** 26823–26829

Wei X, Su X, Cao P, Liu X, Chang W, Li M, Zhang X, Liu Z (2016) Structure of spinach photosystem II-LHCII supercomplex at 3.2 Å resolution. Nature **534:** 69–74

Xu P, Tian L, Kloz M, Croce R (2015) Molecular insights into zeaxanthin-dependent quenching in higher plants. Sci Rep **5:** 13679

Yamamoto HY, Higashi RM (1978) Violaxanthin de-epoxidase: lipid composition and substrate specificity. Arch Biochem Biophys **190:** 514–522

Yang C, Kosemund K, Cornet C, Paulsen H (1999) Exchange of pigment-binding amino acids in light-harvesting chlorophyll a/b protein. Biochemistry **38:** 16205–16213

Zhang L, Melø TB, Li H, Naqvi KR, Yang C (2014) The inter-monomer interface of the major light-harvesting chlorophyll a/b complexes of photosystem II (LHCII) influences the chlorophyll triplet distribution. J Plant Physiol **171:** 42–48

Zhang L, Paakkarinen V, van Wijk KJ, Aro EM (1999) Co-translational assembly of the D1 protein into photosystem II. J Biol Chem **274:** 16062–16067

Downloaded from on October 18, 2017 - Published by www.plantphysiol.org
Copyright © 2017 American Society of Plant Biologists. All rights reserved.